[논 문] 한국재료학회지
Korean Journal of Materials Research
Vol. 5, No. 2 (1995)

Effects of Mo Additions on the Room-Temperature Deformation Behavior of Polysynthetically Twinned (PST) Crystals of TiAl

Myung-Hoon Oh, Min-Chul Kim* and Dang-Moon Wee*

Dept. of Materials Science and Engineering, Kum-Oh National University of Technology
*Dept. of Materials Science and Engneering, KAIST

오명훈 · 김민철* · 위당문*

금오공과대학교 재료공학과
*한국과학기술원 재료공학과

Abstract The effects of Mo additions on the microstructure and the room temperature deformation behavior of polysynthetically twinned (PST) crystals of TiAl were studied in order to get a basic conception for alloying additions on the two-phase TiAl cmpounds with the lamellar structure. It was found that the Mo additions in TiAl PST crystals increase both the yield stress and tensile elongation to fracture but the increase in yield stress depend on the angle ϕ at which the lamellar boundaries lie from the loading axis. The large difference in yield stress between specimens deformed parallel ($\phi=0^{\circ}$) or perpendicular($\phi=90^{\circ}$) to the loading axis and those deformed in intermediate orientations could be explained by the difference in Mo content between the TiAl and the Ti_3Al phases. It was also found that the Mo-doped specimens with intermediate orientation fail by cracking zigzag across to the lamellar boundaries, which is the same fracture mode as that of binary specimens with intermediate orientations tested in vacuum. This suggests that Mo atoms are thought to play a role to reduce the environmental embrittlement of binary PST crystals, resulting in increasing the tensile ductility.

1. INTRODUCTION

Intermetallic compounds based on TiAl/Ti_3Al two-phase alloys have been expected to be one of the most promising candidates for light-weight high-temperature structural materials to replace conventional Ti alloys and some classes of nickel-based superalloys[1-4]. This is because the two-phase TiAl has a attractive properties such as high melting point, high strength-to-weight ratio and excellent oxygen and creep resistance relative to conventional superalloys and titanium-based alloys. One of the major limitations for practical use of this compounds is the poor ductility at ambient temperatures. In the last few years, therefore, a great number of alloying studies have been made on TiAl intermetallic compounds in order to improve its ductility at ambient temperatures (for reviews, see 5). As a results, alloying additions of V, Mn and Cr have been found to raise the room temperature ductility of two-phase TiAl compounds with the duplex structure, while no significant effects on not only single-phase Al-rich TiAl but also two-phase TiAl with the fully lamellar structure[6-8]. It was also proposed that the effect of alloying additions on the room temperature ductility of two-phase TiAl compounds with the duplex form would be explained in terms of changes in tetragonality and unit cell volume[9-11], site occupation[9,12-13], decreasing stacking fault energy and promoting twinning deformation[14-16] and changes in electronic structure[17]. However, it is very difficult to separate the effect of alloying additions from effects resulted from changes in the phase equilibria of the system caused by the alloying

additions. In fact, for example, the grain size of two-phase TiAl compounds has been found to decrease with decreasing aluminium content and with additions of V, Mn and Cr[9-11]. Since the room temperature ductility of two-phase TiAl compounds is sensitive to Ti/Al ratio and the associated microstructure type and grain size[7-8], careful studies are necessary in order to interpret the effect of alloying additions.

Recently, we have succeeded in growing ternary polysynthetically twinned (PST) crystals† of TiAl with a small content of molybdenum, in which only a single grain with the two-phase TiAl/Ti_3Al lamellar structure is contained, by floating zone melting method. With the use of these crystals, we have made a systematic study on the microstructural features and room temperature deformation behavior of Mo-doped ternary PST crystals of TiAl both in tension and compression. The purpose of this paper is to report the effects of Mo additions on the microstructure and room temperature deformation behavior of PST crystals of TiAl in order to get a basic conception for alloying additions on the two-phase TiAl compounds with the lamellar structure.

2. EXPERIMENTAL

The composition of the master ingots used in the present study was Ti-48.4 at.%Al-0.6 at.%Mo. Mo-doped PST crystals, 10 mm in diameter and 70 mm long, were grown from the master ingots using as ASGAL FZ-SS35W optical floating zone furnace at a growth rate of 5 mm/hr under the Ar gas flow. The microstructures of as-grown crystals were studied by optical microscopy and transmission electron microscopy (TEM). Additionally, atom location by channeling enhanced microanalysis (ALCHEMI) experiments were carried out in order to determine the Mo atom sites.

Oriented compression specimens with five different orientations (A_1-D_1 and N in Fig. 1 (a)) and oriented tensile specimens with two

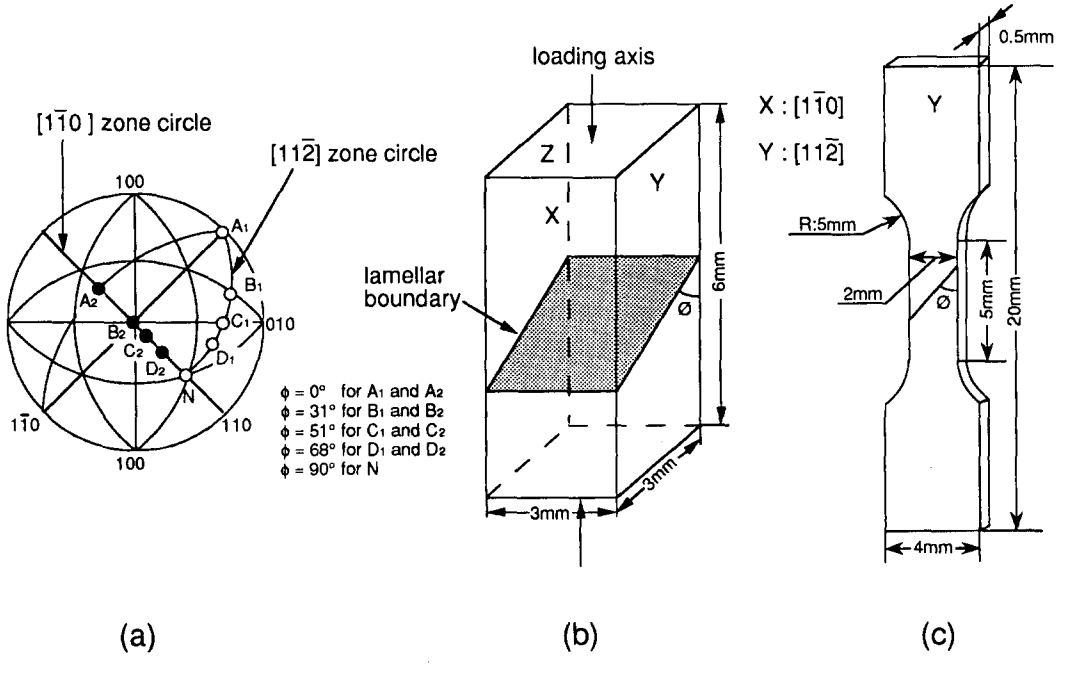

Fig. 1. (a) Stereographic projection of compression and tension axis orentations and (b), (c) geometry and dimensions of compression and tensile specimens, respectively.

† Since numerous thin twin lamellae are contained in the major constituent TiAl phase, we call these crystals *polysynthetically twinned (PST) crystals* by analogy with the phenonenon *polysynthetic twinning* which is often in mineral crystals[20].

different orientations (A_2 and B_2 in Fig. 1(a)), were cut from as-grwon crystals by spark machining. The geometry and dimensions of compression and tensile specimens are shown in Fig. 1 (b) and 1(c), respectively (for details, see 18 and 19). Such specimens were polished first mechanically and then electrolytically in a solution of perchloric acid, n-butanol and methanol to remove surface damage. Compression and tensile tests were carried out on an Instron-type testing machine at a strain rate of 2.0×10^{-4} s^{-1} at room temperature. Deformation structures of compression and tensile specimens were examined by optical microscopy and TEM. Optical microscope observations were made using Nomarski interference contrast.

	TiAl(a)	Ti_3Al(b)
Ti	49.87	61.24
Al	49.39	37.59
Mo	0.74	1.17

(at%)

Fig. 2. EDX analysis of chemical composition in a Mo-doped TiAl PST crystals.

3. RESULTS

3.1 The composition and microstructures of as-grown crystals

A typical microstructure of as-grown Mo-doped TiAl PST crystals revealed by TEM is shown in Fig. 2. The thin foil was cut parallel to the $\{1\bar{1}0\}$ planes which are perpendicular to the (111) lamellar boundary planes. The lamellar boundaries are seen to be flat and parallel to both the $(111)_{TiAl}$ and $(0001)_{Ti_3Al}$ planes. Each TiAl lamella has a thickness in the ranges of 0.5-2.0 μm, and Ti_3Al lamellae with a thickness of about 0.5 μm are separated by some TiAl lamellae and exist every about 10μm, which are almost same as those of binary TiAl PST crystals[21]. Therefore, any significant difference in thickness of TiAl and Ti_3Al lamellae is not observed for Mo-doped TiAl PST crystals.

To determine the composition of as-grown Mo-doped TiAl crystals, energy dispersive X-ray spectrometer (EDX) analysis using analytical electron microscopy (AEM) was made on TiAl lamellae (marked by A) and Ti_3Al lamellae (marked by B), and the results are presented in the bottom of Fig. 2. As seen in the figure, the concentration of molybdenum in Ti_3Al phase is higher than that in TiAl phase. This might be due to the difference in solubility of Mo between the TiAl phase and the Ti_3Al phase. However, the solubility of Mo in the TiAl and the Ti_3Al phases is not clear at present because no detailed Ti-Al-Mo ternary phase diagram is available, especially at ambient temperatures.

Typical microstructures of as-grown binary and Mo-doped PST crystals revealed by optical microscopy observations are shown in Fig. 3(a) and 3(b), respectively. The optical microscope observations were made on the $\{11\bar{2}\}$ planes, which are perpendicular to the lamellar boundary planes. The specimens were chemically etched after electropolishing to reveal the domain structure of the TiAl phase in the lamellar structure. It has been reported in the previous paper that the dark regions in the figure have a plane normal of $[11\bar{2}]$ while the bright regions have a plane normal of either $[1\bar{2}1]$ or $[\bar{2}11]$, so that the contrast corresponds to the difference between the crystallographic orientations of the TiAl domains[21]. As seen in the figure, the size of dark regions in Fig. 3 (b) seems to be smaller than that in Fig. 3

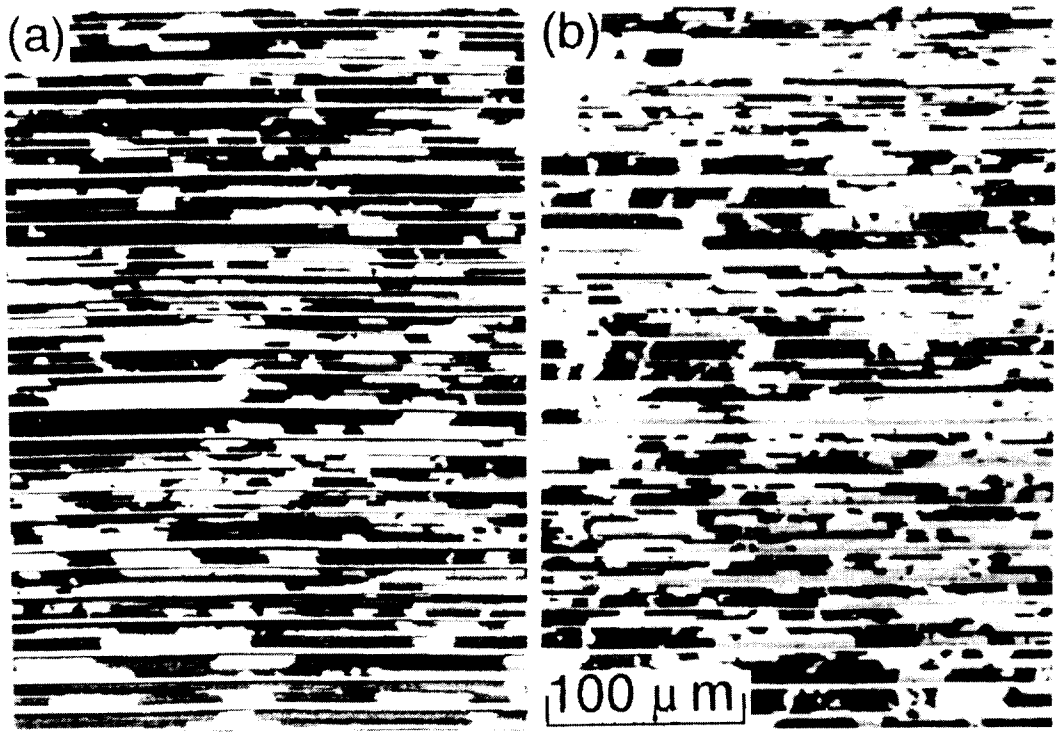

Fig. 3. The domain structure of (a) binary and (b) Mo-doped PST crystals.

(a). In fact, the average size of the dark regions in Fig. 3(b) is about 25 μm in the direction parallel to the lamellar boundaries, while that in Fig. 3 (a) is about 60 μm. The effects of domain size on deformation behavior of TiAl PST crystals will be discussed later in section 4.1.

3.2 ALCHEMI experiments

The ALCHEMI(Atom Location by Channeling Enhanced Microanalysis) technique is a useful method to determine impurity atom sites in a host compounds with a known structure[22]. The basic principle of ALCHEMI is as follows; when a electron beam forms a standing wave inside a crystal, characteristic X-rays are emitted from the crystal, then the location of impurity atoms can be determined by utilizing the emitted X-ray spectra (for details, see 22). Recently, it has been well demonstrated that the atom site of ternary elements in TiAl compounds could be determined by using this ALCHEMI technique[12,13,23].

In the present study, ALCHEMI experiments were carried out to determine the Mo atom sites, and the X-ray spectra and intensities obtained are presented in Fig. 4. The character s in the figure is the deviation parameter from Bragg angle, which indicates that the reflecting angle is deviated from Bragg angle at positive ($s>0$) and at negative ($s<0$), respectively. As seen in Fig. 4, the X-ray intensity from Al for $s>0$ is higher than that for $s<0$. The X-ray intensity from Mo is also higher for $s>0$ than $s<0$ like Al. Accordingly, the ratio of the Mo intensity to the Ti intensity I_{Mo}/I_{Ti} increases with increasing the I_{Al}/I_{Ti} and vise versa. Therefore, from these results, it could be found that Mo atoms are mainly located on the Al sites.

3.3 Deformation behavior in compression

Fig. 5. shows stress-strain curves obtained for specimens with orientations A_1-D_1 (group-1) and N in compression. The yield stress exhibited by these specimens is also strikingly dependent on the angle ϕ at which the lamellar boundaries lie from the compression axis, as

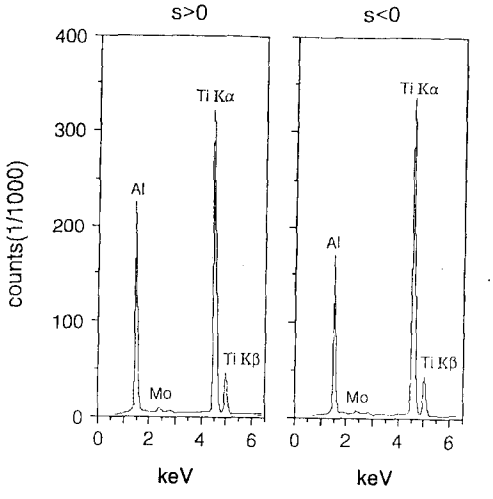

Region	Condition	Intensity			I_{Al}/I_{Ti}	I_{Mo}/I_{Ti}
		I_{Al}	I_{Ti}	I_{Mo}		
I	s>0	146552	297521	3786	0.493	0.0127
	s<0	125333	294000	3119	0.426	0.0106
	non-channel	140371	297403	3641	0.472	0.0122
II	s>0	161794	304732	3987	0.531	0.0131
	s<0	117639	301085	3237	0.391	0.0108
	non-channel	144538	300138	3681	0.482	0.0123

Fig. 4. X-ray spectra and experimental results obtained for Mo-doped TiAl PST crystals by ALCHEMI technique.

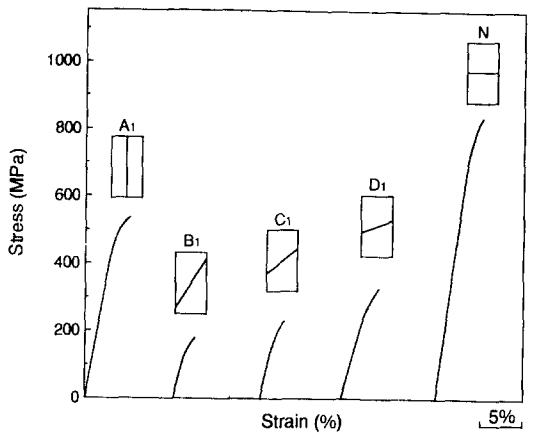

Fig. 5. Typical stress-strain curves obtained for Mo-doped specimens with group-1 otientations in compression.

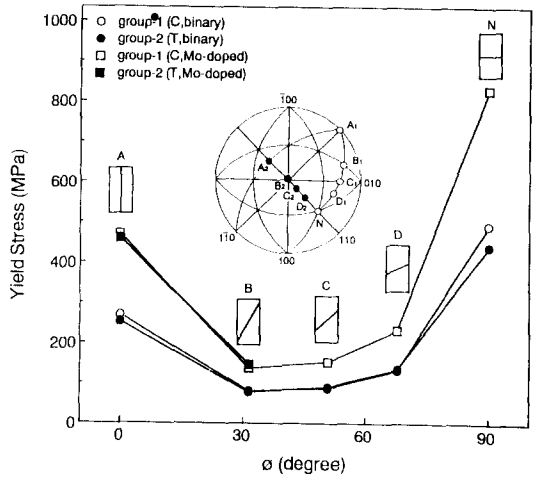

Fig. 6. Yield stress of binary and Mo-doped TiAl PST crystals in compression as a function of the angle ϕ.

the case of binary TiAl PST crystals[18,19]. It is high when the lamellar boundaries are parallel ($\phi=0°$) or perpendicular ($\phi=90°$) to the compression axis and low for intermediate angles. The values of yield stress obtained for Mo-doped specimens with five different orientations are plotted in Fig. 6 as a function of the angle ϕ. The values of yield stress in Fig. 6 are average of three different specimens tested in compression. The values of yield stress obtained for binary specimens, which were already reported in the previous paper[24], are also presented in the figure for comparison. As seen in Fig. 6, Mo-doped specimens show larger values of yield stress than those of binary specimens in all test orientations, although the general trend of orientation(ϕ) dependence of yield stress is almost same in both specimens. It is noteworthy that the ratio of the values of yield stresses obtained for Mo-doped specimens to those of binary specimens is found to be about two times in all test orientations.

Deformation structures revealed by optical microscopy on Mo-doped specimens in compression were found to be very similar to those observed on binary specimens, as shown in Fig. 7. In specimens with orientations A_1 and N, the hard type of deformation, i.e. shear deformation across the lamellar boundaries occurs in both binary and Mo-doped specimens (Fig. 7(a)-(d)), while the easy type of deformation, i.e. shear deformation parallel to the

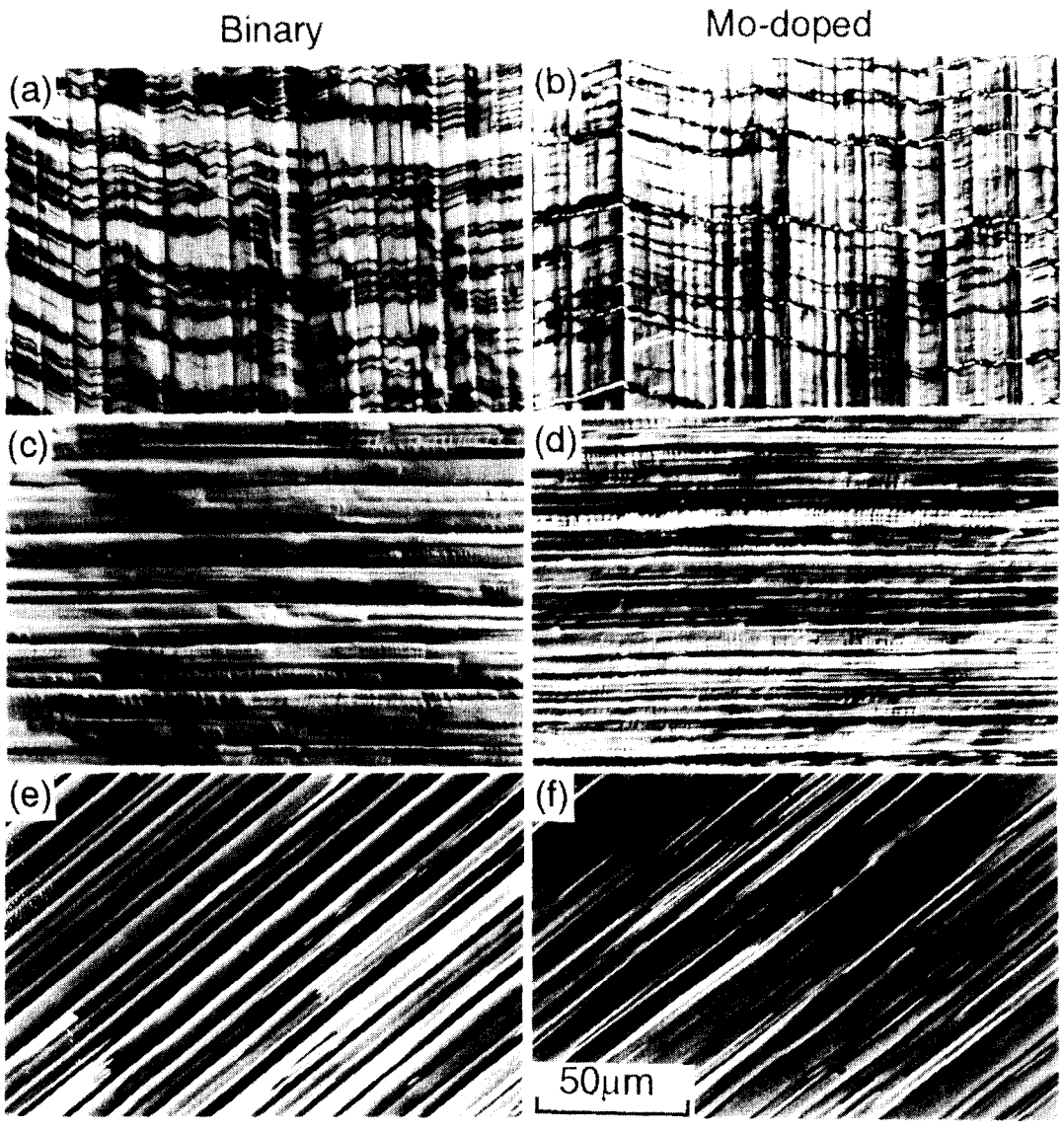

Fig. 7. Deformation markings on the surfaces of binary (a,c,e) and Mo-doped (b,d,f) TiAl PST crystals deformed in compression: (a), (b); A_1, [110]; (c), (d) N, [111]; (e), (f) C_1 [021].

lamellar boundaries occurs when tested in orientations with intermediate angles (Fig. 7(e) and (f))[18,24]. Therefore, as far as optical microscope observations are concerned, any significant difference in deformation structures between binary and Mo-doped specimens does not exist.

3.4 Deformation behavior in tension

To examine the effects of Mo addition on the tensile ductility of TiAl PST crystals, the tensile deformation behavior was investigated for specimens with two different orientations A_2 and B_2, in which the hard and the easy types of deformation occur, respectively. All the specimens were deformed to fracture at room temperature in air at a strain rate of 2.0×10^{-4} s^{-1}. The obtained values of yield stress in tension are plotted in Fig. 8 as a function of the angle ϕ together with those in compression. The values of yield stress obtained for

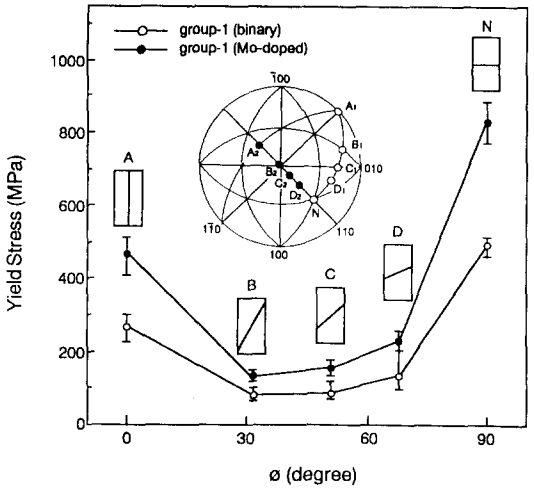

Fig. 8. Yield stress of binary and Mo-doped TiAl PST crystals in tension and compression as a function of the angle ϕ.

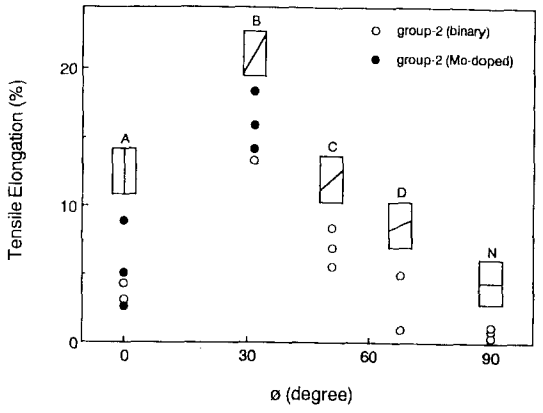

Fig. 9. Elongation to fracture of binary and Mo-doped TiAl PST crystals as a function of the angle ϕ.

Mo-doped specimens are average of three different specimens tested in tension. The average values of yield stress for binary specimens in tension and compression are also presented for comparison[19,24]. As seen in Fig. 8, the average values of yield stress in tension are almost two times higher than those of binary specimens both in orientations A_2 and B_2. Moreover, as seen in Fig. 8, any particularly significant difference in yield stress between tension and compression does not exist. The same results were also observed in the binary TiAl PST crystals[19]. Deformation structures revealed by optical microscopy on the specimen deformed in tension were found to be very similar to those observed on the specimens deformed in compression (Fig. 7). In specimens with orientation A_2, shear deformation occurs across the lamellar boundaries, while shear deformation parallel to the lamellar boundaries occurs in specimens with orientation B_2[19].

The obtained values of tensile elongation for Mo-doped specimens with two different orientations are shown in Fig. 9, together with those for binary specimens. As seen in Fig. 9, Mo-doped specimens with orientations A_2 and B_2 generally show larger values of elongation than those of binary specimens. The maximum values of elongation in orientation A_2 and B_2 are as large as 9.5% and 18.4% in Mo-doped specimens, respectively, while those in binary specimens are 4.3% and 13.3%, respectively[19]. In case of B_2 orientation, tensile elongation obtained for Mo-doped specimens were always larger than those for binary specimens. However, in case of A_2 orientation, a tensile elongation smaller than that of binary specimens was also observed, as shown in Fig. 9. This suggests that the effect of Mo additions is clearly appeared in B_2 orientation rather than in A_2 orientation.

The fracture mode of Mo-doped specimens with orientation A_2 is essentially similar to that of binary specimens, i.e. by cracking in a zigzag across the lamellar boundaries[19]. However, side views of fracture surfaces of specimens with orientation B_2 show that fracture occurs across to the lamellar boundaries in Mo-doped specimens, while fracture occurs in a cleavage-like mode with a habit plane parallel to the lamellar boundaries in binary specimens, as shown in Fig 10 (a) and (b), respectively. Such a mode as that observed in Mo-doped specimens with orientation B_2 are also found to occur when binary specimens with B_1 orientation are tested in vacuum[25]. The environ-

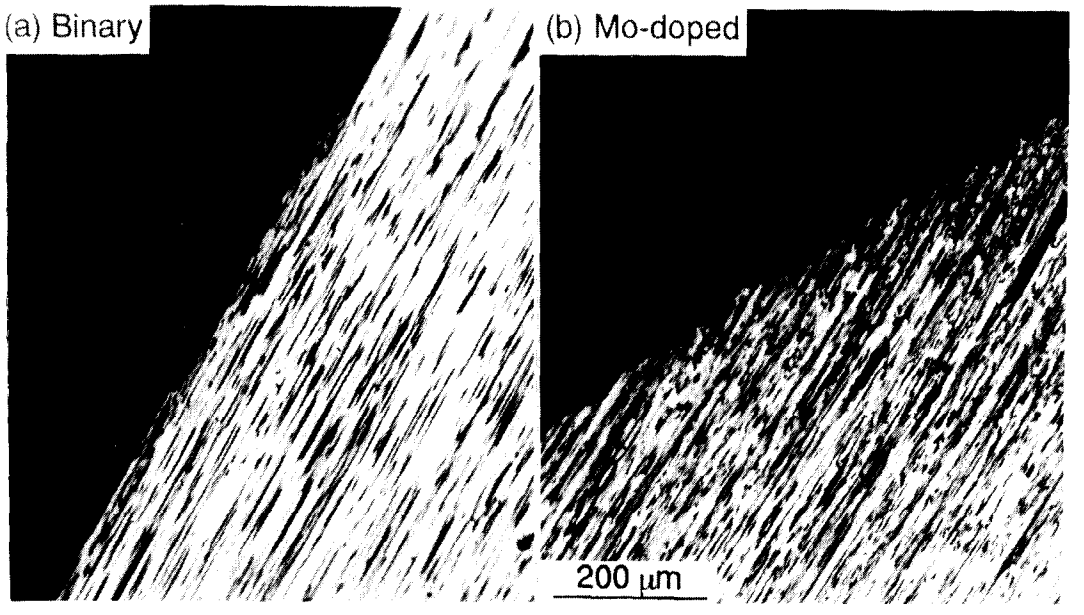

Fig. 10. Side views of fracture su[illegible]es of 9a) binary and (b) Mo-dloped specimens with orientation B_2 tested in air.

mental loss in tensile elongation of binary PST crystals is very large in this orientation. Therefore, it can be supposed that the increase in tensile ductility of Mo-doped specimens with orientation B_2 is related to the change in fracture mode.

4. DISCUSSION

Recently, Huang and Hall have reported that the yield stress of binary two-phase TiAl compounds decreases by as large as 50 MPa when the aluminium content increases from 48 at.% to 49 at.%, and the tensile elongation of binary two-phase TiAl compounds is almost the same in the range of 48-50 at.%Al[26]. This feature is now commonly accepted. In the present study, however, both the yield stress and tensile elongation of Mo-doped TiAl PST crystals have been found to increase, even when the net aluminium content decreases from 49.3 at.%Al to 48.4 at.%Al. This suggests that the results obtained are mainly caused by Mo additions. Therefore, in the present section, the effects of Al content are not discussed.

4.1 Yield strength

In the present study, it is obvious that the yield stress of Mo-doped TiAl PST crystals is higher than that of binary TiAl PST crystals in all test orientations, although the general trend of orientation (ϕ) dependence is almost the same in both crystals. If the increased yield stress obtained for Mo-doped TiAl PST crystals is entirely caused by the solid solution hardening of Mo additions, the increasing values of yield stress must be the same in all test orientations. However, this does not seem to be the case. As seen in Fig. 6, the increasing values of yield stress in orientations A_1 and N are 203 MPa and 336 MPa, respectively, while those in intermediate orientations are 57 MPa (B_1), 69 MPa (C_1), and 99 MPa (D_1), respectively. Therefore, the increasing values of yield stress in orientations A_1 and N are much higher than those in intermediate orientations. This suggests that the difference in the increase in yield stress is related with its deformation type. It is high in orientations deformed by the hard type of deformation (A_1 and N) while it is low in orientations deformed by the easy type of deformation (B_1, C_1 and D_1).

It has been reported in the previous paper that four types of boundaries which cause

resistance to the propagation of shear deformation exist in TiAl PST crystals due to the presence of six different types of ordered domains in the TiAl phase with the lamellar structure; (1) TiAl/Ti_3Al interphase boundaries, (2) true-twin type TiAl/TiAl domain boundaries, (3) pseudo-twin type TiAl/TiAl domain boundaries and (4) 120° rotational order-fault type TiAl/TiAl domain boundaries[18,21]. All four types of boundaries may cause the resistance to the propagation of the hard type of deformation, whereas only type (4) boundaries are relevant when the easy type of deformation occurs[18]. In addition, type (1) boundaries have caused considerable resistance to propagation of deformation[18]. As seen in Fig. 2, the concentration of Mo in the Ti_3Al phase is higher than that in the TiAl phase. Since hardening caused by Mo additions is thought to be much higher in Ti_3Al phase rather than in TiAl phase, the resistance of the Ti_3Al phase to the propagation of the hard type of deformation also increases, causing much increase in yield stress. On the other hand, in intermediate orientations, only type (4) boundaries cause resistance to the deformation propagation. As shown in Fig. 3, the domain size of Mo-doped TiAl PST crystals is smaller than that of binary TiAl PST crystals, resulting in increase of type (4) boundaries. However, as mentioned in the previous paper, type (4) boundaries cause the least resistance since only the direction of shear is changed on the propagation of deformation without changing the shear plane[18]. Therefore, this might be one of the reasons for the difference in the yield stress increase between A_1 and N orientations and intermediate orientations.

4.2 Tensile ductility

Recent studies on alloying additions of third elements have shown that Mn additions enhance the room temperature ductility of two-phase TiAl compounds by promoting twin deformation[9,14,15]. As mentioned previously, however, the principal deformation mode of TiAl PST crystals is deformation twinning of the $\{111\}<11\bar{2}]$† -type while slip along $<1\bar{1}0]$ is the complementary mode to the deformation twinning. To see whether this point of view is true or not, the deformation structures of Mo-doped PST crystals were carefully examined by TEM. Fig. 11 shows an example of the examination conducted in specimens deformed in compression by the easy type of deformation (B_1) and the hard type of deformation (N). Thin foils were cut parallel to the lamellar boundaries in both specimens so that the beam direction was parallel to $<110>_{TiAl}$. As seen in Figs. 11(a) and (b), no significant different in deformation structures was observed in both specimens. That is, the major deformation modes of Mo-doped TiAl PST crystals are deformation twinning of the $\{111\}<11\bar{2}]$-type and slip along $<1\bar{1}0]$ both in specimens deformed by the easy type and the hard type of deformation. Thus, the increase in tensile ductility of Mo-doped TiAl PST crystals cannot be ascribed to the change in deformation mode.

In section 3.4, it was clearly seen that fracture occurred across to the lamellar boundaries in Mo-doped specimens with orientation B_2 which is the same fracture mode as that of binary specimens with B_1 orientation tested in vacuum[25]. Therefore, the increase in tensile ductility by additions of Mo seems to be related to the environmental embrittlement of TiAl PST crystals. As described in the previous paper, binary TiAl PST crystals have shown the hydrogen embrittlement[25], and those with orientation B_1 can be explained by a decohesion model in which the bonding strength along the lamellar boundaries is lowered in the presence of hydrogen gas[25,27,28]. In atomistic calculations of planar faults using interatomic potentials, the relaxation allowing displacements

† The mixed notation $\{hkl\}$ and $<uvw]$ are used to differentiate the first two indices from the third (non-equivalent) index of the tetragonal structure.

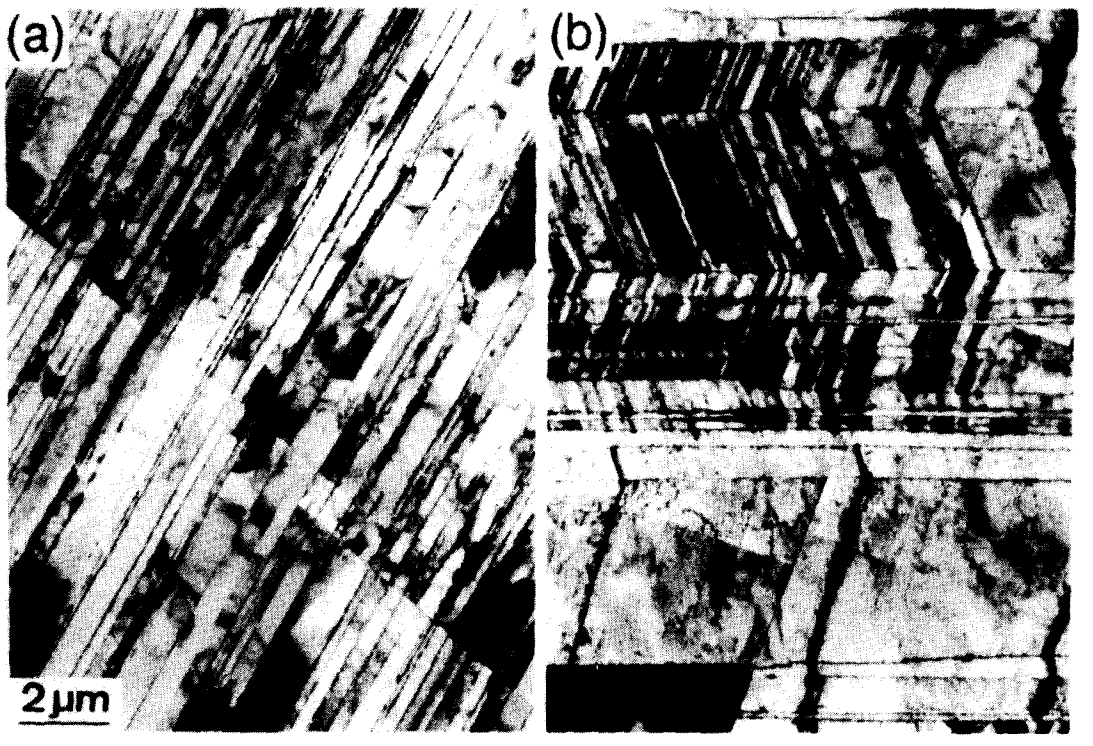

Fig. 11. Deformation structures in Mo-doped specimens with orientation (a) B_1 and (b) N deformed in compression.

of the atoms in the close vicinity to the fault plane often significantly reduces the energies of planar faults. Such displacements of atoms are expected to occur at the boundaries of the pseudo-twin and the 120° rotational types in the TiAl phase. The lamellar domain boundaries of the pseudo-twin and the 120° rotational types involiving such considerable relaxations of atoms are thought to have potential to accept hydrogen along them, offering the preferential path for hydrogen penetration. Then, the bond strength of these boundaries will be reduced in the presence of hydrogen, resulting in a cleavage-like fracture along them, that is, parallel to the lamellar boundaries. The environmental embrittlement in TiAl PST crystals with orientation B_1 can thus be understood in terms of the high susceptibility of the pseudo-twin and 120° rotational lamellar domain boundaries to hydrogen attack. However, these lamellar domain boundaries should have potential to accept not only hydrogen atoms but also ternary alloying atoms. In fact, in the present study, Mo-doped PST crystals of TiAl with orientation B_2 vary in the room temperature fracture mode from the cleavage-like cracking parallel to the lamellar boundaries to cracking zigzag across the lamellar boundaries, and their environmental embrittlement is reduced as a result. This may be because Mo atoms segregate preferentially to the pseudo-twin and 120° rotational lamellar domain boundaries and reduce their vulnerability to hydrogen attack. Recently, the same results as those obtained for Mo-doped TiAl PST crystals have been obtained by addition of ternary elements such as Cr and Mn on TiAl PST crystals[5,29]. Therefore, it could be concluded that the addition of Mo is found to reduce the environmental embrittlement and enhance the room temperature ductility of TiAl PST crystals.

As described in section 3.2, Mo atoms are mainly occupied in Al sites, and this feature is

thought to have also some relation to increasing tensile ductility of TiAl PST crystals. To clarify this effects, however, further studies on changes in tetragonality and electron structure are necessary. The relevant study are now in progress.

5. CONCLUSIONS

Deformation behavior of Mo-doped polysynthetically twinned crystals (PST) of TiAl was studied at room temperature both in tension and compression in order to clarify the effects of third element additions. The results obtained are summarized as follows.

(1) The Mo atoms are mainly occupied in Al sites, and the Mo content in the Ti_3Al phase is higher than in the TiAl phase.

(2) The size of TiAl domains existing in TiAl lamellae is reduced by Mo additions. However, any significant difference in thickness of TiAl and Ti_3Al lamellae is not observed.

(3) The Mo additions in TiAl PST crystals increases both the yield stress and tensile elongation to fracture. However, the increasing values of yield stress depend on its lamellar orientation.

(4) The large difference in yield stress between specimens deformed parallel or perpendicular to the loading axis and those deformed in intermediate orientations is explained by the difference in Mo content between the TiAl and Ti_3Al phases.

(5) The Mo-doped PST crystals with B_2 orientation fail by cracking zigzage across to the lamellar boundaries. This fact suggests that Mo atoms play a role to reduce the environmental embrittlement of binary PST crystals, leading to enhance the tensile ductility.

Acknowledgements

This research was supported by cooperative research fund under "The Korean-Japanese Cooperative Science Program" from the Korea Science and Engineering Foundation.

The authors would like to thank Professor M. Yamaguchi and Dr. H. Inui, Kyoto University, for their help in carrying out the experimental work and grateful discussions.

REFERENCES

1. H. Lipsitt, *High-Temperature Ordered Intermtallic alloys*, MRS Symp. Proc. **39.** (1985), p. 351.
2. M. Yamaguchi, and Y. Umakoshi, *Prog. Mater. Sci.*, **34**, 1 (1990).
3. Y.W. Kim and D.W. Dimiduk, JOM, **43**, 40 (1991).
4. C.T. Liu, *High-Temperature Ordered Intermetallic alloys 5*, MRS Symp. Proc. **288** (1993), p. 3.
5. M. Yamaguchi and H. Inui, *Structural Intermetallics*, ed. R. Daloria et al. TMS, Warrendale, Pa (1993), p. 127.
6. Y. W. Kim, *High-Temperature Ordered Intermetallic alloys 4*, MRS Symp. Proc. **213** (1991), p. 777.
7. E. L. Hall, and S. C. Huang, *Microstructure /Property Relationships in Titanium Aluminides and Alloys*, ed. Y. W. Kim et al. TMS, Warrendale, Pa (1991), p. 47.
8. Y. W. Kim and F. H. Froes, *High Temperature Aluminides and Intermetallics*, ed. S. H. Whang *et al.* TMS, Warrendale, Pa (1990), p. 465.
9. T. Tsujimoto and K. Hashimoto, *High-Temperature Ordered Intermetallic alloys 3*, MRS Symp. Proc. **133** (1989), p. 391.
10. S. C. Huang and E. L. Hall, *High-Temperature Ordered Intermetallic alloys 3*, MRS Symp. Proc. **133** (1989), p. 373.
11. T. Kawabata, T. Tamura and O. Izumi, *High-Temperature Ordered Intermetallic alloys 3*, MRS Symp. Proc. **133** (1989), p. 329.
12. S. C. Huang and E. L. Hall, *Acta metall. mater.*, **39**, 1053 (1991).
13. S. C. Huang and E. L. Hall, *Metall. Trans.*, **22A**, 2619 (1991).
14. T. Hamamura, R. Uemori and T. Tamino,

J. Mater. Res., **3**, 659 (1988).
15. T. Hanamura and T. Tamino, *J. Mater. Sci. Lett.*, **8**, 24 (1989).
16. G. Hug and P. Veyssiere, Intl. Symp. Proc. on *Electron Microscopy in Plastic and Fracture Research of materials*, Dresden, Oct. 8-13 (1989).
17. M. Morinaga, J. Saito, N. Yukawa and H. Adachi, *Acta metall. mater.*, **38**, 25 (1990).
18. H. Inui, A. Nakamura, M. H. Oh and M. Yamaguchi, *Phil. Mag. A*, **66**, 557 (1992).
19. H. Inui, M. H. Oh, A. Nakamura and M. Yamaguchi, *Acta metall. mater.*, **40** 3095 (1992)
20. C. S. Barrett and T. B. Massalski, *Structure of Metals*, 3rd ed., pp. 406, Pergamon Press, Oxford (1980).
21. H. Inui, M. H. Oh, A. Nakamura and M. Yamaguchi, *Phil. Mag. A*, **66**, 539 (1992).
22. J. C. Spence and J. Tafto, *J. Microsc.*, **130**, 147 (1983).
23. D. Shindo, M. Hirabayashi, T. Kawabata and M. Kikuchi, *J. Electron Microsc.*, **35**, 409 (1986).
24. T. Fujiwara, A. Nakamura, M. Hosomi, S. R. Nishitani, Y. Shirai, and M. Yamaguchi, *Phil. Mag. A*, **61**, 591 (1990).
25. M. H. Oh, H. Inui, M. Misaki and M. Yamaguchi, *Acta metall. mater.*, **41**, 1939 (1993).
26. S. C. Huang and E. L. Hall, *Metall. Trans.* **22A**, 427 (1991).
27. C. T. Liu and C. G. McKamey, *High Temperature Aluminides and Intermetallics*, ed. S. H. Whang *et al.* TMS, Warrendale, Pa (1990), p. 133.
28. N. S. Stoloff, M. Shea and A. Castagna, *Environmental Effects on Advanced materials*, ed. R. H. Jones *et al.* TMS, Warrendale, Pa (1991), p. 3.
29. M. H. Oh, H. Inui, M. Misaki, M. Kobayashi and M. Yamaguchi, *High-Temperature Ordered Intermetallic Alloys 5*, MRS Symp. Proc. **288** (1993), p. 1001.